Structure, Vol. 9, 1165–1181, December, 2001, ©2001 Elsevier Science Ltd. All rights reserved. PII S0969-2126(01)00687-6

Interdomain Interactions in Hinge-Bending Transitions

Neeti Sinha,[1,5] Sandeep Kumar,[2] and Ruth Nussinov[1,3,4]
[1]Intramural Research Support Program
Science Applications International Corporation and
[2]Laboratory of Experimental and Computational Biology
National Cancer Institute-Frederick
Building 469, room 151
Frederick, Maryland 21702
[3]Sackler Institute of Molecular Medicine
Department of Human Genetics and Molecular Medicine
Sackler Faculty of Medicine
Tel Aviv University
Tel Aviv 69978
Israel

Summary

Background: The mechanisms that allow or constrain protein movement have not been understood. Here we study interdomain interactions in proteins to investigate hinge-bending motions.

Results: We find a limited number of salt bridges and hydrogen bonds at the interdomain interface, in both the "closed" and the "open" conformations. Consistently, analysis of 222 salt bridges in an independently selected database indicates that most salt bridges form within rather than between independently folding hydrophobic units. Calculations show that these interdomain salt bridges either destabilize or only marginally stabilize the closed conformation in most proteins. In contrast, the nonpolar buried surface area between the moving parts can be extensive in the closed conformations. However, when the nonpolar buried surface area is large, we find that at the interdomain interface in the open conformation it may be as large or larger than in the closed conformation. Hence, the energetic penalty of opening the closed conformation is overcome. Consistently, a large nonpolar surface area buried in the closed interdomain interface accompanies limited opening of the domains, yielding a larger interface.

Conclusions: Short-range electrostatic interactions are largely absent between moving domains. Interdomain nonpolar buried surface area may be large in the closed conformation, but it is largely offset by the area buried in the open conformation. In such cases the opening of the domains appears to be relatively small. This may allow prediction of the extent of domain opening. Such predictions may have implications for the shape and size of the binding pockets in drug/protein design.

[4]Correspondence: ruthn@ncifcrf.gov (Bldg. 469, Rm. 151, NCI, Frederick, MD 21702)
[5]Present address: Basic Research Laboratory, Building 469, Room 110, National Cancer Institute at Frederick, Maryland 21702.

Introduction

In solution, proteins exist in an ensemble of conformational isomers. The distribution of the conformers is a function of the degree of their molecular flexibility and of external conditions in which they reside. Most mutational variants manifest only small fluctuations, corresponding to a relatively smooth landscape. On the other hand, molecules exhibiting larger flexibility may be described by funnels with rugged bottoms, with the extent of the ruggedness corresponding to their range of flexibility. Hinge-bending motions may be considered to manifest relatively rugged bottoms, with low barriers separating the minima wells. The low barriers, corresponding to low energy transitions, enable the molecules to flip and interconvert between the different "open" and "closed" conformations. Hence, there is no need to invoke an *induced fit* mechanism to rationalize binding to an incoming ligand. The conformer that is most favorable for binding is the one that is selected [1, 2], with the low energy barriers enabling the equilibrium to straightforwardly shift in the direction of this conformer and in this way propagate the binding reaction. A similar behavior is observed during crystallization. The conformer that crystallizes is not necessarily the one with the highest population time in solution. However, it is the most favorable for binding to sister conformers under these conditions, with the equilibrium shifting in its favor.

Since hinge-bending transitions involve low barriers, here our goal is to investigate the types of interactions between the moving parts. For this purpose, we utilize the database of motions [3]. Through analysis of fragment, domain, and subunit motions we illustrate that although in the closed conformations the non-polar buried surface area between the moving parts can be quite large, the number of salt bridges and hydrogen bonds is small, or they are absent altogether. This is in agreement with the relative insensitivity of hinge-based motions to sequence variability at the interdomain interface. It is well known that families of proteins manifest similar hinge-bending motions. There are a number of well-studied examples, such as the flap movements in aspartic proteases [4–8], the kinases, and the cytokine receptor superfamily [9]. Consistently, analysis of similar architectures has illustrated that molecular hinges tend to recur at similar sites, despite the sequence variability [4, 10]. Combined, these analyses argue that the swiveling motion is probably not determined by the details of the atomic interactions. Hydrophobic interactions have long been postulated to be involved in plasticity, i.e., in generating a broad range of conformational isomers, whereas salt bridges and hydrogen bonds have been suggested to impart specificity and rigidity. Hence, the nonspecific hydrophobic interactions may be extensive in folding and in binding; however, close-range electrostatic interactions are largely avoided between moving domains.

Key words: domain movements; interdomain interactions; hinge-bending; population shifts; electrostatic interactions

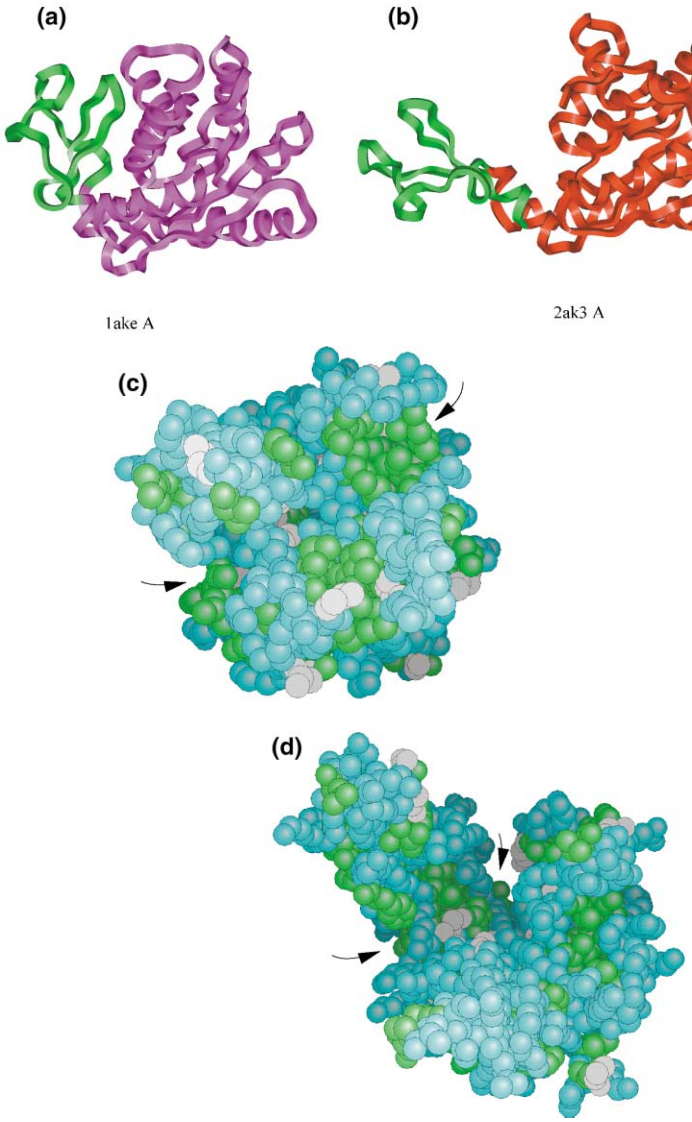

Figure 1. The Closed and Open Conformations of Adenylate Kinase

For the closed (a,c) conformation the PDB coordinate file 1ake A is used. The open conformation (b,d) is taken from 2ak3 A. (a) and (b) depict the backbone, clearly showing the large hinge-bending motion which takes place. The hinging domain is shown in green. (c) and (d) illustrate the surface area types (non-polar surface areas are green, polar areas in cyan). The figure has been generated using GRASP [60]. The hinges are marked by arrows.

The limited occurrence of electrostatic interactions between the domains is consistent with our recent analysis of the sequence separation between salt bridges. Salt bridges tend to occur within, rather than between, building blocks, with most of them separated by fewer than 50 residues [11]. We have further analyzed 222 nonequivalent salt bridges in 36 nonhomologous monomeric proteins whose high-resolution crystal structures are available in the protein data bank (PDB) [12] with respect to their occurrence within and across hydrophobic folding units (HFU). We find that most salt bridges in our database are intra-HFU salt bridges. Only 16 are inter-HFU salt bridges. The inter-HFU salt bridges have similar electrostatic strengths as the intra-HFU ones, largely because of their geometries and environments.

Furthermore, for the domain motion cases in which both the closed and open conformations exist in the database, we also analyzed the open conformations. We find that here too the number of salt bridges and hydrogen bonds is limited or nonexistent. On the other hand, the nonpolar surface area buried between the domains in the open conformation is either larger or about the same as that buried between the domains in the closed conformation, compensating for the energy penalty paid by opening the domains. Figure 1 depicts adenylate kinase as an example of a hinge-bending motion. The movement of the domains is observed clearly in Figures 1a and 1b. The polar and non-polar surface areas in the closed and the open conformations are shown in Figures 1c and 1d. In adenylate kinase, the area buried between the domains in the closed conformation is relatively small (650 Å^2). On the other hand, Figures 2a and 2b show the closed and open conformations of glutamate dehydrogenase. Here, the nonpolar surface area buried between the domains is substantially larger in the closed conformation (2587 Å^2). In the open conformation, however, it is even larger (4677 Å^2), owing to the rearrangement of the molecule, as clearly observed in the figure. Interestingly, in adenylate kinase the movement is larger (Figure 1b), with a larger distance between the domains (11 Å in adenylate kinase and 0.6 Å in glutamate dehydrogenase). This behavior recurs in

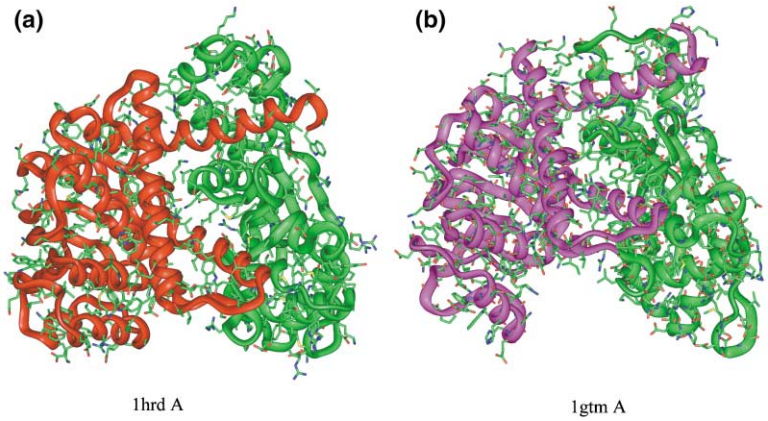

Figure 2. Hinge-bending movements in glutamate dehydrogenase

The hinge-bending domain is shown in green. (a) 1hrd A and (b) 1gtm A are the 'closed' and 'open' conformations respectively. The side-chains are displayed to highlight the extensive interface between the hinge-bending domains. The side-chains are colored atom-wise. The figure illustrates the extensive rearrangement of the open *versus* the closed conformation.

the other cases, suggesting that to overcome the large hydrophobic energy opposing the opening, a substantial nonpolar surface area should also be buried in the open conformation. Clearly, this is more straightforwardly achieved if the movement is not too large.

Previous Hinge-Bending Analyses: Detection and Packing

Most studies of hinge-bending motions focus on the determination of the location of the hinge. This is most frequently accomplished with structural comparisons and the use of either rigid or flexible algorithms to allow hinge bending [13–20]. Methods originally developed for analyzing domain motions from simulations [21] have been adapted and extended for prediction and analysis of X-ray conformers of proteins with more than two domains [22]. Recently, an alternate approach to predicting the hinge and the modes of motions has also been devised [23].

Previously, two potential factors had been examined in analyses of hinge-bending motions, packing and residues at, or next to, hinge-bending sites. With regard to preferences for single, pairs, or triplets of residues at/next to hinge-bending sites, recent experiments have shown that this is apparently not the case, although some residues are avoided, either because they allow too much swiveling (like Gly), or because they hinder hinge-bending motions [24]. On the other hand, a correlation between packing and hinge-bending movements has been detected, although owing to backbone, and in particular to side-chain movements that optimize packing, it has been unclear as to whether the motions are the outcome of the looser packing or whether a looser packing is observed because motion has taken place.

Packing has been very convenient for a systematic classification of protein motions [3, 25]. Packing has been selected as the basic criterion because atoms are well packed in the interior of the protein molecule. Groups of atoms can move with respect to each other only if there is a packing defect, or a cavity, that enables them to do so. Interfaces between groups of atoms or between structural parts are not smooth. Interdigitation, particularly of side chains, imposes constraints on movements of structural units if their internal packing is to be preserved. In hinge-bending motions the structural units move with respect to each other; however, whereas the packed arrangement within the unit is largely conserved, the packing at their interface is disrupted. Swiveling on their "hinge," the parts move as relatively rigid bodies with respect to each other. The motion that is observed is roughly perpendicular to the interface. Hinge-bending movements differ from those classified as "shear." In shear movements the packing at the interface is maintained, with the structural units sliding with respect to each other. Additionally, whereas in hinge-bending movements a few large (twisting) changes may be observed, in shear movements many small changes, parallel to the plane of the interface, may be seen [25]. Here we confine ourselves to hinge-bending motions because they are more common. Such movements may be observed between small structural parts, such as loops or secondary-structure elements, between hydrophobic folding units, or between domains. Hence, they can be intramolecular if they are connected by the backbone of the polypeptide chain, or they can be intermolecular. Thus, in this sense too, intra- and intermolecular associations resemble each other [2, 26]. The only exception is that owing to chain connectivity in intramolecular hinge motions, there are additional constraints on the movements imposed by the covalently linked polypeptide chain.

Results

Our analysis of the interdomain interactions has been carried out on all 25 cases in the molecular motions database for which protein structures were available both in the open and in the closed conformations. The criteria for choosing the cases from the motions database were 2-fold. First, the motion must be characterized as hinge in the literature (in the original crystal structure papers) or have been assigned as such by the algorithm used to construct the database [3]. Second, using both Insight and the Geometric Hashing structural comparison, we have visually examined all superimposed structural pairs and picked cases that showed clear movement. Most of the structural pairs that were consistent with the first criterium were used in the analysis.

Table 1. Hydrogen Bonds and Salt Bridges between Moving Parts in Closed Conformations

Protein	ID (size)	Hinging Region[a]	Salt Bridges[b]	H Bonds[bc]		
				M-M	M-S	S-S
Fragment Motions						
YP tyrosine phosphatase	1yts (278)	151–159	0 (6)	1 (113)	5 (94)	1 (27)
Triosephosphate isomerase	1tti (243)	166–176	0 (5)	1 (112)	2 (46)	0 (12)
Lactate dehydrogenase	1ldm (329)	96–110	0 (4)	1 (167)	1 (65)	0 (13)
Triglyceride lipase	4tgl (269)	83–96	1 (6)	0 (103)	3 (69)	1 (14)
Annexin V	1avr (320)	183–191	0 (11)	1 (235)	0 (63)	1 (22)
HIV-1 protease	4hvp A (99)	33–62	0 (1)	3 (21)	1 (14)	0 (3)
Seryl-tRNA synthetase	1ser B (421)	28–98	1 (10)	1 (199)	0 (69)	0 (39)
Domain Motions						
Lactoferrin	1lfg (691)	90–251	0 (12)	0 (270)	2 (176)	6 (36)
Adenylate kinase	1ake A (214)	121–159	0 (7)	1 (116)	4 (37)	0 (19)
Calmodulin	2bbm A (148)	82–148	0 (7)	0 (54)	1 (15)	0 (0)
Lysozyme	1l96 (164)	*N*–59	2 (4)	0 (104)	0 (38)	3 (11)
Maltodextrin BP	1anf (370)	*N*–109	0 (6)	0 (199)	3 (82)	1 (13)
Phosphoglycerate kinase	13pk A (415)	5–194	1 (9)	0 (187)	0 (108)	3 (21)
TBSV coat protein	2tbv C (387)	67–266	0 (5)	0 (57)	0 (55)	0 (8)
Troponin C	1tnw (162)	*N*–90	0 (1)	0 (92)	0 (15)	0 (0)
DNA polymerase β	2bpg A (335)	*N*–87	0 (6)	0 (138)	0 (75)	0 (18)
Glutamate dehydrogenase	1hrd A (449)	*N*–200	0 (12)	1 (267)	0 (28)	0 (28)
Recoverin	1rec (201)	*N*–78	1 (11)	0 (119)	2 (49)	2 (15)
Tryptophan synthase	1bks B (397)	93–189	1 (11)	0 (206)	2 (79)	1 (25)
Protein kinase	1ctp E (350)	40–127	0 (2)	0 (132)	9 (64)	1 (12)
Subunit Motions						
ATCase (5at1)	A (310), B (153)	A (310)	2 (10)	1 (168)	4 (109)	4 (33)
Glycogen (9gpb) phosphorylase	A (842), B (842)	A (842)	0 (52)	0 (703)	10 (330)	3 (129)
Phosphofructokinase (6pfk)	AB (638), CD (638)	AB (638)	0 (11)	0 (540)	4 (295)	7 (65)
Hemoglobin (4hhb)	A (141), B (146)	A (141)	0 (11)	0 (437)	18 (123)	9 (42)
Lac repressor (1lbi)	A (360), B (360)	A (360)	0 (15)	0 (294)	2 (97)	4 (22)

The electrostatic interaction at the interdomain interface in the closed conformation. The sizes of the proteins are in parentheses, following the PDB codes. M-M: main chain-main chain hydrogen bond. M-S: main chain-side chain hydrogen bond. S-S: side chain-side chain hydrogen bond. In parentheses are the number of salt bridges and hydrogen bonds found in the whole protein.

[a] The region that moves with respect to the rest of the protein. The residue positions of the hinging regions are shown.

[b] The number of salt bridges and hydrogen bonds at the interface of the hinging region and the rest of the protein in fragment and domain movement cases, and at the interface of subunits in subunit movements.

[c] Hydrogen bonds.

Interactions in the Interdomain Interface in the 'Closed' Conformations

Table 1 lists the number of salt bridges and hydrogen bonds present at the interfaces of the closed conformations. The moving fragments are in the range of 8–29 residues, except in Seryl-tRNA synthetase, where it is 70 residues long. Only a few salt bridges connect the moving fragments to the remainder of the protein, even though the overall number of such interactions in the proteins is significant. Similarly, there are relatively few hydrogen bonds connecting the moving fragments to the rest of the protein. These observations also hold for domain and subunit movements. The size of the moving domains ranges from 45 to 200 residues. They have few, if any, salt bridges or hydrogen bonds connecting them to the rest of the protein, with significantly higher numbers in the whole proteins. In the cases of subunit movements, the subunits are in the range of 141–842 residues, also with few salt bridges or hydrogen bond connectors.

Table 2 lists the calculated nonpolar buried surface areas for these cases. The nonpolar buried surface areas at the interface of the domains in the closed conformations are significantly smaller as compared to the areas buried within their corresponding domains. This holds also for subunit movements. In the category of fragment movements, however, in a few cases such as 1yts, 1tti, 1ldm, and 1avr the nonpolar surface area buried at the interface is larger than that buried within the fragments. In these cases the fragment is a coil.

Interactions in the Interdomain Interface in the 'Open' Conformations

Tables 3 and 4 list the corresponding values for the open conformations. Here we have carried out the calculations only for those cases that are classified as domain motions and in which both closed and open conformations, including full sequence, identifier, and complete coordinate files of the same chains, are available. Table 3 provides the electrostatic interactions. Inspection of the table indicates a situation similar to that observed in Table 1, namely, a limited number of salt bridges and hydrogen bonds at the interface. The exception is the number of main chain-side chain hydrogen bonds at the interface of glutamate dehydrogenase, which, as seen in Table 4 and Figures 2a and 2b, is large (14 H bonds). However, the number of intradomain hydrogen bonds

Table 2. Nonpolar Buried Surface Area at the Interfaces in Closed Conformations

Protein	The Hinging Region	Non-polar buried surface area		
		Total[a] (Å^2)	Intra[b] (Å^2)	Inter[c] (Å^2)
Fragment Motions				
1yts (278)	151–159	1170	443	1042
1tti (243)	166–176	1190	647	885
1ldm (329)	96–110	1352	773	903
4tgl (269)	83–96	1247	896	536
1avr (320)	183–191	810	385	547
4hvp A (99)	33–62	3113	2496	1194
1ser B (421)	28–98	6706	6376	595
Domain Motions				
1lfg (691)	90–251	18273	17831	1010
1ake A (214)	121–159	3622	3178	650
2bbm A (148)	82–148	5820	5619	258
1l96 (164)	*N*–59	6162	5353	1679
1anf (370)	*N*–109	12775	11166	3973
13pk A (415)	5–194	21289	20560	1789
2tbv C (387)	67–266	19962	19342	620
1tnw (162)	*N*–90	8227	8165	108
2bpg A (335)	*N*–87	8050	7912	256
1hrd A (449)	*N*–200	21150	21502	2587
1rec (201)	*N*–78	8425	7919	1110
1bks B (397)	93–189	10593	9167	2526
1ctp E (350)	40–127	10564	8447	4177
Subunit Motions				
5at1	A (310), B (153)	34574	34227	830
9gpb	A (842), B (842)	99220	97434	3035
6pfk	AB (638), CD (638)	72192	70450	3364
4hhb	A (141), B (146)	14519	13986	1158
1lbi	A (360), B (360)	32850	31281	2935

The nonpolar surface area buried between domains in the closed conformation (see Table 4 for the open conformation). Fragment, domain, and subunit motion cases are given. In Table 4, only domain hinge-bending cases are presented. The hinges as assigned in the database of molecular movements (DMM) [3] have been utilized for the present analysis. The open and closed conformations are used to estimate the rotation and translation accompanying the molecular movements [47] (see Experimental Proceudres). To see the extent of molecular movements we have calculated the bend and twist angles as well as the differences in interdomain distances associated with domain movements. The distances are for the closed-open and thus yield negative values. The more negative the value, the larger the opening. We have utilized the program FlexProt [20] for this purpose. FlexProt is an efficient tool for automatically comparing two flexible structures without specifying the location of the hinge. FlexProt detects corresponding rigid domains that superimpose with a small RMSD and finds the flexible regions simultaneously. On the other hand, DMM superimposes only the static core [47]. Since the two algorithms detect moving domains by different procedures, the locations of the hinging domains utilized for the bend, twist, and interdomain distance calculations might be slightly different than those assigned in DMM. For example, in the case of glutamate dehydrogenase, a domain from residue position 28 to 188 was compared with a domain from residue position 189 to 257 for the bend, twist, and inter-domain distance calculations, while a domain from residue position 1 to 200 was compared with the rest of the protein (201–449) in the rest of the analysis. However, for most of the cases the hinging domains were similar in the two procedures. Additionally, for the bend and twist angles and the changes in interdomain distance evaluation, we have selected the hinges closest to hinges in DMM [3]. The residue positions of the hinging regions are shown.

[a] Total nonpolar buried surface area of the hinging region.

[b] Nonpolar buried surface area within the hinging region.

[c] Nonpolar buried surface area at the interface of the hinging regions and the rest of the protein in fragment and domain motions, as well as between subunits in subunit motions.

is also much larger (101 in the open conformation as compared to 28 in the closed conformation), owing to the rearrangement that took place. Such rearrangements, which are reflected in different numbers of intradomain electrostatic interactions, are also observed in other cases. Figure 3a presents a chart of the inter- versus the intradomain short-range electrostatic interactions in the closed and open conformations.

Table 4 presents the nonpolar surface areas buried between the domains in the open conformations. Inspection of the table illustrates that for most cases, the nonpolar buried surface area in the open conformation is either larger (considerably larger for glutamate dehydrogenase, see Figures 2a and 2b) or roughly similar, with a difference of 50–80 Å^2. Such a difference suggests movements of a few residue side-chain atoms. For example, Gly buries 85 Å^2, Asp 151 Å^2, and Arg 241 Å^2 [27]. For troponin C (108 Å^2 in the closed conformation and 52 Å^2 in the open conformation) and for DNA polymerase β (256 Å^2 in the closed conformation and 112 Å^2 in the open conformation), the nonpolar buried surface is twice as large for the closed as for the open conformation, but these values and their differences are relatively small. The histograms in Figure 3b illustrate the differences in the nonpolar buried surface areas in the closed versus the open conformations.

Table 3. Hydrogen Bonds and Salt Bridges between Hinge-Bending Domains in Open Conformations

Protein	The Hinging Region[a]	Salt Bridge[b]	Hydrogen Bonds[bc]		
			MC-MC	MC-SC	SC-SC
Lactoferrin (1lfh)	90–251	0 (10)	1 (265)	1 (194)	0 (25)
Adenylate kinase (2ak3 A)	121–159	0 (5)	0 (105)	0 (43)	0 (13)
Calmodulin (1cll)	82–148	0 (1)	0 (103)	0 (57)	0 (1)
Lysozyme (1l97)	*N*–59	0 (5)	0 (103)	0 (36)	5 (13)
Troponin C (1ncx)	*N*–90	0 (4)	0 (111)	0 (62)	0 (11)
DNA polymerase β (1bpd)	*N*–87	0 (4)	0 (143)	0 (47)	0 (15)
Glutamate dehydrogenase (1gtm A)	*N*–200	0 (14)	0 (220)	14 (101)	5 (33)
Recoverin (1iku)	*N*–78	0 (2)	0 (88)	1 (21)	0 (1)
Trypotophan synthase (1ttp A)	93–189	0 (2)	0 (139)	2 (41)	1 (10)
Protein kinase (1apm E)	40–127	0 (4)	1 (150)	18 (75)	2 (16)

The electrostatic interaction at the interdomain interface in the open conformation. The sizes of the proteins are in parentheses, following the PDB codes. The sizes of the proteins are in parentheses, following the PDB codes. M-M: main chain-main chain hydrogen bond. M-S: main chain-side chain hydrogen bond. S-S: side chain-side chain hydrogen bond. In parentheses are the number of salt bridges and hydrogen bonds found in the whole protein.

[a] The region that moves with respect to the rest of the protein. The residue positions of the hinging regions are shown.

[b] The number of salt bridges and hydrogen bonds at the interface of the hinging region adn the rest of the protein in fragment and domain movement cases, and at the interface of subunits in subunit movements.

[c] Hydrogen bonds.

Using the standard desolvation energy penalty of 25 cal/Å^2, one could conclude that a hydrophobic energy of between 3 (in troponin C) and 65 (in glutamate dehydrogenase and in tryptophan synthase) kcal/mol would oppose the opening of the domains. On the other hand, this penalty is either compensated for or overcome in the open conformation by larger contributions, between 1.3 (in troponin C) and either 117 kcal/mol (in glutamate dehydrogenase) or 74 kcal/mol (in tryptophan synthase).

It is interesting to relate the column in Table 4 of interdomain nonpolar buried surface areas in the closed conformation (and its associated energy column) with that for the difference in the distances between the closed and the open conformations. With the exception of troponin C, if the nonpolar surface area buried between the domains in the closed conformation is small (less than 650 Å^2 in Table 4), the distance is large (here 11–19 Å). On the other hand, if the nonpolar surface area buried between the domains in the closed conformation is large (1000–2600 Å^2, in Table 4) the distance is much smaller (between 0.6 and 5.0 Å). The troponin C exception could possibly be the outcome of the higher stability of the interdomain helix, as compared to that of calmodulin. We have carried out linear regressions of the change in interdomain nonpolar surface area between the closed and open conformations ($\Delta ASA_{inter}^{nonpolar} = ASA_{inter\text{-}closed}^{nonpolar} - ASA_{inter\text{-}open}^{nonpolar}$) in the ten proteins (in Table 4) with the three hinge-movement parameters (i.e., bend, twist, and distance). When normalized by the interdomain nonpolar surface area in the open conformation ($ASA_{inter\text{-}open}^{nonpolar}$), $\Delta ASA_{inter}^{nonpolar}$ indicates a correlation with the distance, with a linear correlation coefficient of 0.6. A Student's t test shows that this correlation is significant at the 95% level of confidence but not at the 99% level.

We have further computed the total nonpolar buried surface areas of both conformations for each of the cases (Table 5 and Figure 3b). We have normalized these values by the size (which sometimes varies because the same molecule has not always has been crystallized in both conformations). The calculations have been performed with our in-house program [28]. Inspection of Table 5 and Figure 3b reveals that in all cases either the total nonpolar buried surface areas are roughly similar in the closed versus the open conformation or they are larger for the open conformation. However, the overall differences in the total (or per residue) values in the open as compared to the closed conformation are small. Taken together, the results from Tables 1–4 (and Figure 3) suggest that the population times of the open conformations may be higher than those for the closed. Nevertheless, these results do not rule out the possibility of cases in which the closed conformer would be more stable than the open. In such cases, the closed conformation would have a higher population time in solution. However, through a population shift brought about by the stabilizing effect of ligand binding, the binding reaction would propagate. Inspection of the table further illustrates that the per-residue values are roughly constant, regardless of the protein size. Although not observed here, possibly because of the small number of protein cases, one may further expect that the per-residue energy will decrease as the protein size increases since packing of larger molecules is less optimal than that of the smaller ones.

Electrostatic Strengths of Salt Bridges and Ion Pairs

The Hinge-Bending Motion Cases

Electrostatic interactions play important roles in protein structure and function, for example in oligomerization, molecular recognition, allosteric regulation, domain motions, flexibility, thermostability, and α helix capping [29–36]. The strength of an electrostatic interaction between two charged residues depends mainly upon three factors, namely, the location of the charged residues in the protein, the geometrical orientation of the side-chain charged groups with respect to each other, and the interaction of the two charged residues with the other charges in the protein [11].

We have computed the strengths of salt bridges

Table 4. Nonpolar Buried Surface Area at the Interfaces in Open Conformations as Compared to Closed Conformations

Protein	Hinging region	Nonpolar Buried Surface Area (Å²)				Hydrophobicity[d] (Inter Kcal/mol)		Movement		
		Total[a]	Intra[b]	Inter[c]						
				Closed	Open	Closed	Open	Bend[e]	Twist[f]	Distance[g]
Lactoferrin (1lfh)	90–251	17,734	17,115	1,010	1,249	−25.250	−31.225	−20.874	−30.790	−4.532
Adenylate (2ak3 A) kinase	121–159	3,876	3,509	650	584	−16.250	−14.600	−45.359	85.513	−11.149
Calmodulin (1cll)	82–148	6,011	5,905	258	186	−6.450	−4.650	−84.170	−34.672	−14.835
Lysozyme (1l97)	*N*–59	6,272	5,545	1,679	1,625	−41.975	−40.625	−5.00	−2.129	−0.732
Troponin C (1ncx)	*N*–90	8,830	8,805	108	52	−2.700	−1.300	−15.919	57.508	−2.958
DNA polymerase β (1bpd)	*N*–87	7,897	7,820	256	112	−6.400	−2.800	−74.972	28.557	−18.610
Glutamate (1gtm A) dehydrogenase	*N*–200	23,497	21,129	2,587	4,677	−64.675	−116.925	6.925	−1.178	0.593
Recoverin (1iku)	*N*–78	7,657	6,779	1,110	1,931	−27.750	−48.275	−50.760	10.781	−5.248
Trypotophan (1ttp A) synthase	93–189	11,510	10,102	2,526	2,978	−63.150	−74.450	−4.778	−6.495	−5.322
Protein (1apm E) kinase	40–127	12,292	8,225	4,177	4,940	−104.4	−123.5	−17.757	−80.834	−2.046

The nonpolar surface area buried between domains in the open conformation. See the legend for Table 2.

[a] Total nonpolar buried surface area of the hinging region.

[b] Nonpolar buried surface area within the hinging region.

[c] Nonpolar buried surface area at the interface of the hinging regions and the rest of the portein in fragment and domain motions, as well as between subunits in subunit motions.

[d] Hydrophobic contribution at the interface.

[e] Bending angle of the hinging domain when closed and open conformations are compared with FlexProt.

[f] Twisting angle of the hinging domain when closed and open conformations are compared with FlexProt.

[g] The distance between the centroid of the hinging domain and centroid of the rest of the protien, as calculated with FlexProt.

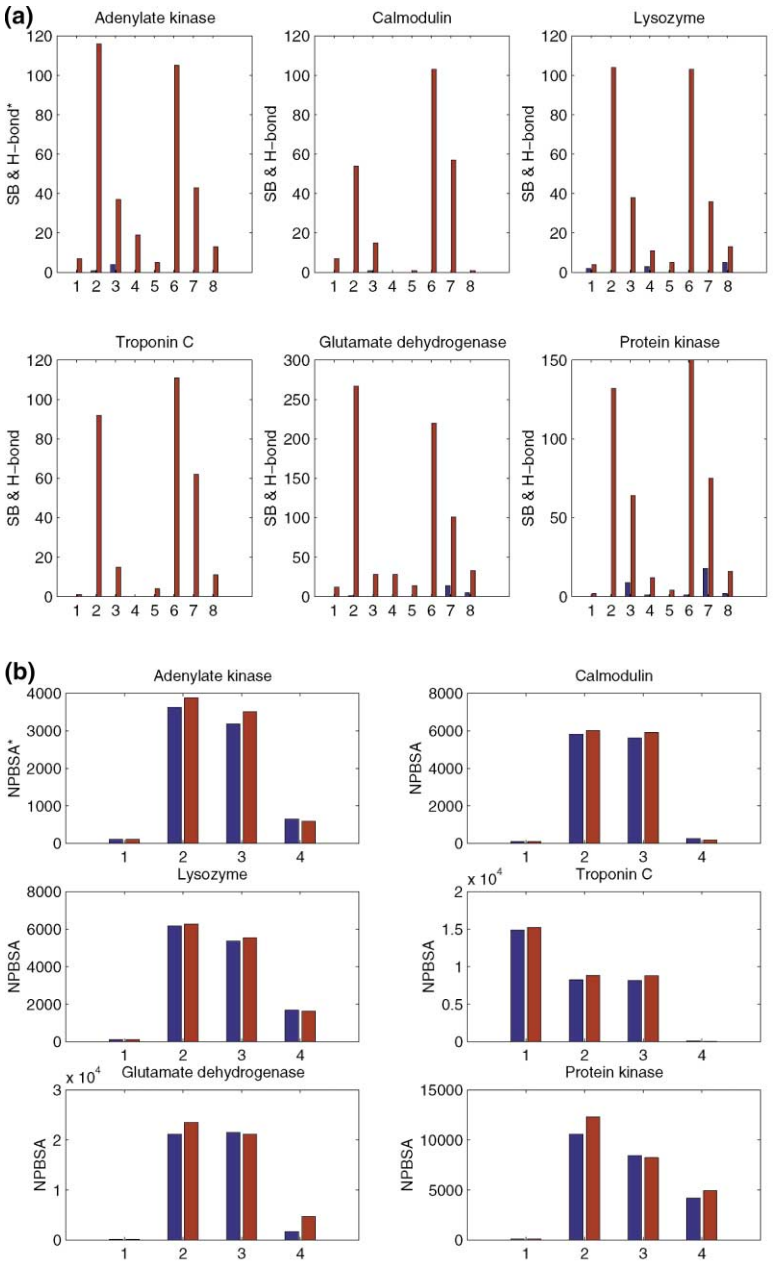

Figure 3. Electrostatic Interactions and Nonpolar Buried Surface Areas in 'Open' and 'Closed' Conformations

(a) Histograms showing the short-range electrostatic interactions in the open versus the closed conformations. The histograms show the number of salt bridges and hydrogen bonds at the hinging-domain interface and in the whole protein. The numbers 1–4 on the *x* axis are the values for the closed conformation, and 5–8 are for the open conformation. Numbers 1 and 5 on the *x* axis show the number of salt bridges. Numbers 2, 3, and 4 (and 6, 7, and 8) are for main chain-main chain, main chain-side chain, and side chain-side chain hydrogen bonds, respectively. Blue bars relate to the interdomain interface, while red bars show the values in the whole protein. A value of 0 indicates that there are no salt-bridges or hydrogen-bonds. See Tables 1 and 3. An asterisk indicates a salt bridge and a hydrogen bond.

(b) The nonpolar buried surface areas in the closed (in blue) versus the open (in red) conformations. Position 1 on the *x* axis is the value for the whole protein, while 2, 3, and 4 are the total nonpolar buried surface area (NPBSA) of the hinging domain, the nonpolar surface area buried within the hinging domain, and the nonpolar surface area buried between the hinging domain and the rest of the protein, respectively.

NPBSA stands for *n*onpolar *b*uried *s*urface *a*rea, in Å^2. In the cases of adenylate kinase, calmodulin, lysozyme, glutamate dehydrogenase, and protein kinase, the nonpolar buried surface area of the protein is shown by the average (normalized) nonpolar surface area buried per residue since the number of residues varies between the closed and the open conformations.

formed between fragments and domains showing hinge-bending motions in the closed conformations. Subunit motions have not been considered for such calculations because of the large protein size. However, intersubunit salt bridges and ion pairs are also expected to behave similarly. As Table 1 shows, the number of interfragment and interdomain salt bridges is small, only seven. Our criteria for salt bridge formation are strict and identify only those with good geometries [11]. This may be one of the reasons for the lower count of interpart salt bridges. We have therefore relaxed our criteria and computed the electrostatic contribution to protein stability of all ion pairs and their networks; we have required only the second criterion, i.e., that oxygen and nitrogen atoms in a pair of oppositely charged side chains be within a 4.0 Å distance, and have neglected the centroid 4.0 Å distance requirement. Table 6 lists the electrostatic strengths of ion pairs and their networks formed across hinge-bending parts in the 25 proteins. Ion pairs satisfying both criteria are shown in bold. There are 15 ion pairs and four ion triads in Table 6. Nine of these 15 are stabilizing, and six are destabilizing. Five of the nine stabilizing ion pairs are weak ($\Delta G_{tot} = -2$ kcal/mol or weaker). Among the four ion triads (consisting of 8 out of the 15 ion pairs), two are destabilizing. The individual component ion pairs in the destabilizing ion triad formed by residues Asp 38, Glu 40, and Arg 100 of tryptophan synthase (1bksB) are also destabilizing. However, this is not the case for the other destabilizing ion triad. The ion triad formed by Asp 356, Arg 404, and Arg 409 in *Yersinia* protein tyrosine phosphatase (1yts) is destabiliz-

Table 5. Total Nonpolar Buried Surface Area in Closed and Open Conformations

		Closed conformation				Open Conformation		
Protein	ID[a] (Size[b])	NPBSA[c] (Å^2)	Normalized NPBSA[d] (Å^2)	Hydrophobicity[e] (kcal/mol)	ID (Size)	NPBSA (Å^2)	Normalized NPBSA (Å^2)	Hydrophobicity (kcal/mol)
Lactoferrin	1lfg (691)	75,363	109	−2.73/res.[f]	1lfh (691)	75431	109	−2.73/res.
Adenylate kinase	1ake A (214)	22,779	106	−2.65/res.	2ak3 A (225)	23676	105	−2.62/res.
Calmodulin	2bbm A (148)	12,406	83	−2.07/res.	1cll (144)	13057	90	−2.25/res.
Lysozyme	1l96 (162)	17,112	105	−2.62/res.	1l97 A (164)	17400	106	−2.65/res.
Troponin C	1tnw (162)	14,871	92	−2.29/res.	1ncx (162)	15236	94	−2.35/res.
DNA Polymerase β	2bpg A (324)	33,801	104	−2.60/res.	1bpd (324)	33646	104	−2.60/res.
Glutamate dehydrogenase	1hrd A (449)	50,207	111	−2.77/res.	1gtm A (417)	48446	116	−2.90/res.
Recoverin	1rec (185)	19,922	107	−2.67/res.	1iku (188)	19954	106	−2.65/res.
Tryptophan synthase	1bks B (392)	43,814	111	−2.77/res.	1ttp A (256)	28454	111	−2.77/res.
Protein kinase	1ctp E (333)	37,723	113	−2.82/res.	1apm E (341)	39277	115	−2.87/res.

The total nonpolar buried surface area and the hydrophobic contributions in the closed and in the open conformations.
[a] PDB codes.
[b] Number of residues.
[c] Nonpolar buried surface area.
[d] In some cases the number of residues is different between the closed and open conformations, as in adenylate kinase, calmodulin, lysozyme, glutamate dehydrogenase, recoverin, tryptophan synthase, and protein kinase, since different proteins were crystallized.
[e] Hydrophobic contributions to folding.
[f] Average hydrophobic contributions per residue.

ing. In the case of the stabilizing ion triad formed by Glu 12, Glu 16, and Lys 84 in recoverin (1rec), one component ion pair is destabilizing and the other is stabilizing. All four interdomain ion pairs and the ion triad formed by Asp 10, Glu 11, and Arg 145 in lysozyme (1l96) are stabilizing. Table 6 shows that in nine (1yts, 4tgl, 3hvp, 1serB, 1lfg, 1akeA, 13pkA, 1rec, and 1bksB) protein chains, the overall close-range electrostatic interactions are either destabilizing or only marginally stabilizing to the closed conformation. Only in the case of lysozyme (1l96) are the electrostatic interactions stabilizing.

Among the 15 ion pairs described above, seven can be classified as salt bridges. Of these seven, four are destabilizing by 2–6 kcal/mol. Despite the fact that the geometries of these four salt bridges are better than those of the remaining eight ion pairs, their bridge energy terms are not strong enough to overcome the large desolvation penalties. In the case of three salt bridges, the protein energy terms are also unfavorable (Table 6). The remaining three (out of seven) salt bridges are stabilizing by −0.5 to −2.3 kcal/mol. Two of the three stabilizing salt bridges are in lysozyme. The third stabilizing bridge is in Seryl-tRNA synthase (1serB). It is only marginally stabilizing ($\Delta\Delta G_{tot} = -0.548$ kcal/mol).

All the interdomain electrostatic interactions in lysozyme are stabilizing. In particular, the ion triad formed

Table 6. Electrostatic Strengths of 15 Interfragment/Domain Ion Pairs and Their Networks in Our Database

Salt Bridge	$\Delta\Delta G_{dslv}$	$\Delta\Delta G_{brd}$	$\Delta\Delta G_{prt}$	$\Delta\Delta G_{tot}$	$\Delta\Delta G_{assoc}$
1yts D356–R404	+7.351	−2.226	−6.614	−1.489	−0.977
1yts D356–R409	+10.188	−3.992	−10.186	−3.990	−0.979
4tgl D61–R86	+3.570	−0.624	+0.008	+2.953	−0.291
3hyp K20–E34	+7.710	−2.522	−4.672	+0.516	−1.255
1serB R508–D534	+9.515	−9.654	−0.409	−0.548	−4.533
1lfg E66–R120	+5.061	−3.530	−1.544	−0.012	−1.751
1akeA D110–K195	+1.737	−1.658	−1.359	−1.281	−1.130
1l96 D10–R145	+19.610	−6.022	−24.788	−11.200	−0.857
1l96 E11–R145	+9.926	−7.201	−4.700	−1.975	−3.805
1l96 E22–R137	+1.234	−3.495	−0.006	−2.266	−2.871
13pkA R65–D222	+6.420	−4.602	+1.796	+3.614	−1.126
1rec E12–K84	+3.222	−2.144	−5.372	−4.294	−0.371
1rec E16–K84	+9.280	−5.726	−0.756	+2.797	+1.553
1bksB D38–R100	+8.040	−3.798	+1.651	+5.894	−2.350
1bksB E40–R100	+5.635	−1.410	+3.421	+7.646	−0.640
1yts R404–D356–R409[a]	+13.695	−4.465	−7.698	+1.532	−1.754
1l96 D10–R145–E11[a]	+21.764	−11.473	−18.936	−8.646	−4.450
1rec E12–K84–E16[a]	+2.806	−5.773	+1.024	−1.943	−4.712
1bksB D38–R100–E40[a]	+5.246	−2.707	−0.200	+2.340	−1.678

Various energy terms in kcal/mol for 15 ion pairs and their networks formed between moving fragments and domains of proteins that show hinge-bending motion. Each ion pair and ion triad is represented by its component residue names and numbers and the PDB entry code. The residue names are given in single-letter code. D, E, H, K, and R stand for Asp, Glu, His, Lys, and Arg, respectively. The quantities denoted by the energy terms are described in the text. The ion pairs that satisfy both our criteria for being classified as salt bridges are shown in bold.
[a] Ion triads are formed when a charged residue interacts with two other charged residues.

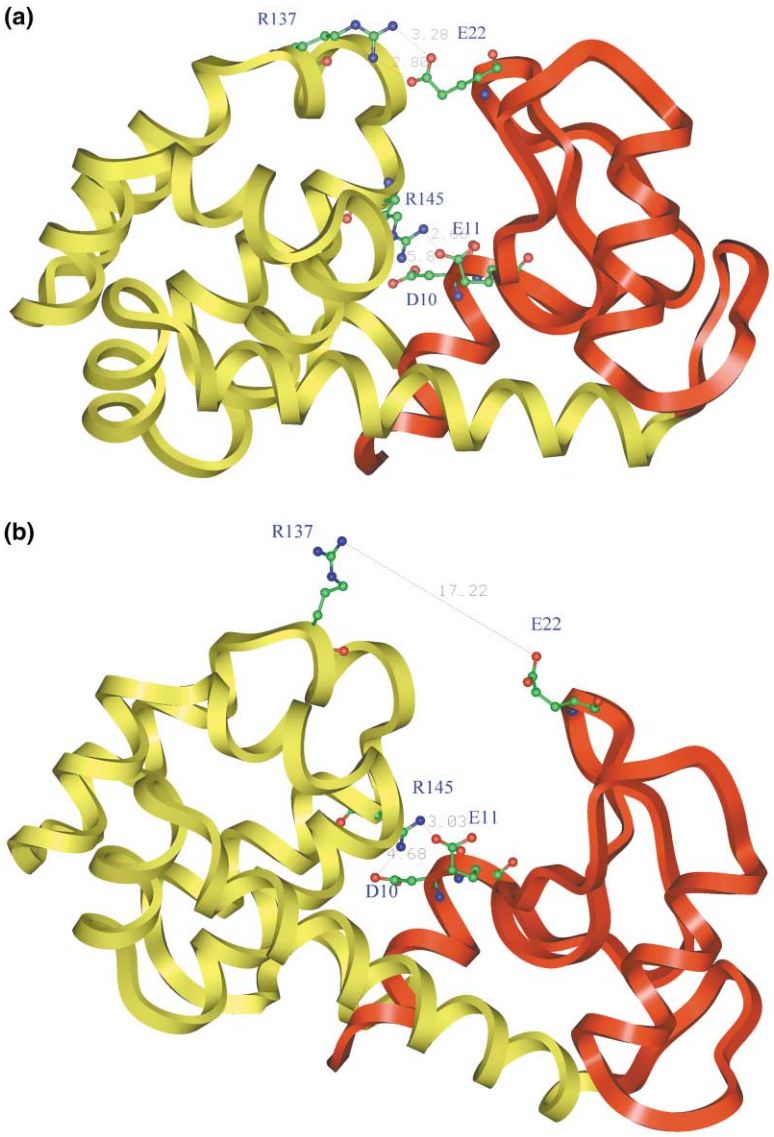

Figure 4. Closed and Open Conformations of T-4 Lysozyme

(a) Closed conformation.
(b) Open conformation
Domains that move relative to each other are shown in red and yellow. The hinge position for the movement lies just after the red region. Residues forming interdomain salt bridges in the closed conformation are shown with their side chains and are labeled. The salt bridge R137-E22 is broken, whereas salt bridges D10-R145 and E11-R145 are retained in the open conformation (b).

by residues Asp 10, Glu 11, and Arg 145 is stabilizing by −8.6 kcal/mol. A comparison of the closed and open conformations of lysozyme shows that this ion triad is preserved in the open conformation. The other salt bridge, formed by Glu 22 and Arg 137, stabilizes the closed conformation by −2.3 kcal/mol and is broken in the open conformation, with the distance between the two charged residues increasing to more than 13 Å. The open and closed conformations of lysozyme are shown in Figure 4, highlighting the positions of Asp 10, Glu 11, Glu 22, Arg 137, and Arg 145.

Inter- and Intra-HFU Salt Bridges

The above observations are based on only 25 cases, in which molecular motions have been observed in the molecular movements database [3]. These available data are sparse, particularly for salt bridges and ion pairs formed across domains and fragments. Under such limited data circumstances, it is useful to analyze an analogous but independent data set and compare the results obtained from the two sets. Our second data set consists of 222 nonequivalent salt bridges from 36 nonhomologous monomeric proteins whose high-resolution (1.6 Å or better) crystal structures are available in the PDB [12]. The salt bridges in this database have been identified by the application of both distance criteria. Hence, these salt bridges have favorable geometries. The 36 proteins are cut into their hydrophobic folding units (HFU) [37]. Hydrophobic folding units are compact, stable substructures with a strong hydrophobic core, which preserves their structures in solution [37]. Here we compare the strengths of the salt bridges formed within and across hydrophobic folding units (HFUs).

Out of the 222 salt bridges, 183 (82.4%) are formed within the HFUs, and 16 (7.2%) are formed across the HFUs. The remaining 23 (10.4%) salt bridges contain at least one residue that falls in a region that is not assigned to any HFU. Sixteen proteins in our database contain more than one hydrophobic folding unit. The total num-

Table 7. Electrostatic Strengths of 16 Inter-HFU Salt Bridges in Our Database of 36 Nonhomologous Protein Monomers

Salt Bridge	$\Delta\Delta G_{dslv}$	$\Delta\Delta G_{brd}$	$\Delta\Delta G_{prt}$	$\Delta\Delta G_{tot}$	$\Delta\Delta G_{assoc}$
153l D41–H75	+10.652	−9.727	−5.024	−4.099	−4.844
1ads D36–K61	+4.748	−7.622	−0.993	−3.867	−5.164
1ads D43–K77	+19.804	−14.475	−9.295	−3.967	−4.210
1aky R132–D168	+17.161	−16.678	−1.719	−1.237	−6.920
1aop R366–E448	+10.964	−12.974	−1.420	−3.430	−7.589
1aru K49–E190	+6.059	−7.750	−3.953	−5.644	−5.544
1aru E176–K279	+5.569	−4.885	−4.747	−4.063	−2.476
1dim R37–E361	+19.268	−11.948	−11.492	−4.172	−3.871
1dim D89–K120	+4.369	−6.577	−2.476	−4.684	−4.648
1edg H254–E307	+17.539	−6.466	−16.792	−5.719	−0.624
1fmk R160–D365	+11.006	−7.781	−7.642	−4.416	−4.203
1smd E27–R387	+20.662	−18.170	−24.936	−22.445	−10.847
1smd D173–K213	+1.980	−4.174	−0.003	−2.196	−3.248
1smd K278–D411	+4.682	−2.323	−6.893	−4.533	−1.139
1smd K322–D485	+9.124	−6.024	−4.147	−1.047	−2.244
3pte E78–R186	+9.522	−6.189	−9.338	−6.005	−3.073

Various energy terms in kcal/mol for 16 inter-HFU salt bridges in our dataset of 36 nonhomologous proteins. Each salt bridge is labeled by the PDB code of the protein and the names and numbers of the residues in the salt-bridging pair. The residue names are given in single-letter code. D, E, H, K, and R stand for Asp, Glu, His, Lys, and Arg, respectively. The quantities denoted by the energy terms are described in the text.

ber of salt bridges in these 16 proteins is 152. Out of these 152, 115 (75.7%) are formed within HFUs (intra-HFU salt bridges), 16 (10.5%) are formed across HFUs, and the remaining 21 salt bridges are in unassigned regions. Of the 16 proteins that contain more than one HFU, six proteins do not contain any inter-HFU salt bridge.

In the whole database of 222 salt bridges, 66 (29.7%) are buried in the proteins, with the average ASA (accessible surface area) for these salt bridges being less than 20%. Similarly, 44 (24.0%) of the 183 intra-HFU salt bridges are buried in the protein. On the other hand, 10 (62.5%) out of the 16 inter-HFU salt bridges are buried (data not shown). Based on the overall distribution of buried and surface-exposed salt bridges in the database of 222 salt bridges, only five (66 $\times$ 16/222) inter-HFU salt bridges are expected to be buried. This increase in proportion of buried inter-HFU salt bridges is significant at the 95% level of confidence [38].

Out of the 183 intra-HFU salt bridges, 153 (83.6%) have stabilizing electrostatic contributions, and the remaining 30 (16.4%) are destabilizing to the protein structures. These observations agree well with those for all the 222 salt bridges in the database. Out of 222 salt bridges in our data set, 190 (85.6%) are stabilizing, and 32 (14.4%) are destabilizing [11]. On the other hand, all 16 inter-HFU salt bridges are stabilizing. Based on the distribution of stabilizing and destabilizing salt bridges in the data set of 222 salt bridges, 14 out of 16 inter-HFU salt bridges are expected to be stabilizing, and the remaining two are destabilizing.

Table 7 lists the electrostatic strengths of the 16 inter-HFU salt bridges in our data set. Table 8 presents the average values of various energy terms for all 222 salt bridges, 183 intra- and 16 inter-HFU salt bridges. Large standard deviations about the average values indicate a large scatter in the data. However, it can be seen that the intra-HFU salt bridges have an average electrostatic contribution that is similar to the average over all 222 salt bridges. On the other hand, inter-HFU salt bridges pay greater desolvation penalties, $\Delta\Delta G_{dslv}$, owing to their larger proportion of burial. Nevertheless, these larger desolvation penalties are overcome by stronger bridge ($\Delta\Delta G_{brd}$) and protein ($\Delta\Delta G_{prt}$) energy terms for the inter-HFU salt bridges. A comparison of the relative magnitudes of the bridge and protein energy terms indicates that the protein energy term ($\Delta\Delta G_{prt}$) contributes toward the stability of inter-HFU salt bridges to a greater extent. Table 8 suggests that inter-HFU salt bridges have greater average stability ($\Delta\Delta G_{tot} = -5.10 \pm 4.84$ kcal/mol) than the intra-HFU salt bridges ($\Delta\Delta G_{tot} = -3.51 \pm 3.79$ kcal/mol). However, this difference is largely due to the inter-HFU salt bridge E27-R387 in 1smd (α-amylase). This salt bridge has high calculated stability (Table 7). If we remove this salt bridge from our list of inter-HFU salt bridges, the average $\Delta\Delta G_{tot}$ for the remaining 15 inter-HFU salt bridges is -3.94 ± 1.48 kcal/mol. Hence, intra- and inter-HFU salt bridges have similar stabilities. The advantages and limitations of the method used for calculating electrostatic strengths of salt bridges and ion pairs have been discussed in detail by Hendsch and Tidor [39] (1994). The purpose of the electrostatic

Table 8. Average Energy Terms in Various Salt Bridge Categories in Our Database of 38 Nonhomologous Protein Monomers

Salt Bridge Class	$\Delta\Delta G_{dslv}$ (kcal/mol)	$\Delta\Delta G_{brd}$ (kcal/mol)	$\Delta\Delta G_{prt}$ (kcal/mol)	$\Delta\Delta G_{tot}$ (kcal/mol)	$\Delta\Delta G_{asso}$ (kcal/mol)
All	+6.54 ± 5.48	−6.34 ± 4.38	−3.86 ± 4.35	−3.66 ± 3.86	−3.64 ± 2.63
Intra-HFU	+6.01 ± 5.12	−5.96 ± 4.20	−3.56 ± 4.09	−3.51 ± 3.79	−3.53 ± 2.64
Intra-HFU	+10.82 ± 6.24	−8.99 ± 4.60	−6.93 ± 6.53	−5.10 ± 4.84	−4.42 ± 2.54

All: the whole data set of 222 salt bridges [11]. Intra-HFU: 183 intra-HFU salt bridges. Inter-HFU: 16 inter-HFU salt bridges.

calculations presented here is to provide qualitative comparisons.

Discussion

Although proteins are inherently flexible molecules, a closer inspection of the structures reveals that some structural parts are more rigid than others. The more rigid parts are likely to be more compactly packed, to have a stronger hydrophobic core, and to have a stronger stabilizing electrostatic contribution. Movements of the backbone of such structural domains, subdomains, or any structural part may conceivably result in large displacements of these structural units. Here we address such large-scale, low-energy-barrier, hinge-bending motions. Such motions are typically included in Koshland's classical so-called *induced fit* model [1, 26, 40]. The larger deviations have enabled the identification of the locations of the hinges [3] and have thereby allowed us to study some of the potential factors playing a role in molecular movements.

Here we have examined three structural factors: the non-polar buried surface area between the moving parts; hydrogen bonds; and salt bridges. The nonpolar buried surface area reflects the hydrophobic effect, the major driving force in protein folding and binding, although to variable extents [28, 41]. On the other hand, salt bridges and hydrogen bonds have been shown to play a larger role in intermolecular binding as compared to folding [31, 42]. On the face of it, we might have expected that the extent of nonpolar buried surface area between moving parts would not be extensive. However, this was not borne out in our calculations.

Inspection of the values of the nonpolar buried surface areas between the moving parts and the rest of the protein reveals that although variable, they can be quite large. On the other hand, the number of salt bridges, or hydrogen bonds, is limited. Our recent analyses of proteins that form amyloids, and of domain swapping cases, have shown a similar behavior [43]. Consistently, our extensive analysis of salt bridges in a nonredundant data set of monomeric proteins has illustrated that the number of salt bridges between independently folding hydrophobic units [37] is relatively small. In particular, in a data set of 36 proteins, containing 222 salt bridges, 183 are formed within hydrophobic folding units, whereas only 16 are formed across the folding units. However, both inter- and intra-hydrophobic-folding-unit salt bridges have similar electrostatic strengths, and both are largely a function of their geometries and environments. In agreement with this observation, we find that ion pairs in NMR conformers with distances of mostly more than 4.0 Å between the corresponding charged groups are largely destabilizing [44]. This suggests that a possible reason for the largely absent salt bridges and hydrogen bonds is the barrier heights that would need to be overcome in hinge-bending motions.

A comparison of the inter-HFU salt bridges with the salt bridges and ion pairs formed across fragments and domains in the 25 proteins that show hinge-bending motion illustrates that whereas all the inter-HFU salt bridges are stabilizing, this is not the case for the inter-domain and inter-fragment salt bridges and ion pairs. Ten out of 15 interdomain and interfragment salt bridges and ion pairs are either destabilizing or only weakly stabilizing ($\Delta\Delta G_{tot} = -2$ kcal/mol or weaker). These observations can be rationalized in two ways. First, inter-HFU salt bridges have better geometry since they satisfy both of the distance criteria mentioned in the Experimental Procedures. On the other hand, among the 15 interdomain/fragment electrostatic interactions, only seven satisfy both criteria. Geometry is an important determinant of salt bridge or ion pair stability [11]. Still, we observe that four of these seven salt bridges are destabilizing. Despite the favorable geometry, the protein environment around these four salt bridges does not support their formation. Second, for all the 25 hinge-bending-motion proteins, there is crystallographic evidence for the protein motion. Of the 16 (out of 36) monomeric proteins that contain more than one HFU, hinge-bending motion has been observed for only five proteins. Three of these five proteins do not contain any inter-HFU salt bridge. The remaining two proteins (PDB entries 1fmk and 1ads) contain a total of three inter-HFU salt bridges.

Hence, our results indicate that most of the salt bridges are formed within the hydrophobic folding units rather than across them. In terms of the final electrostatic strengths, the intra- and inter-HFU salt bridges do not show significant differences. Hence, electrostatic interactions are largely avoided across two parts of a protein. On the other hand, the electrostatic interactions that are observed between the protein parts have strengths similar to those within the protein parts. However, the origin of their stabilizing contributions differs.

Taken together, our results for the cases picked from the database of motions, and for the independent monomer data set, suggest that salt bridges and other ionic interactions are avoided between the moving parts of the proteins, possibly because of kinetic barriers. In cases in which these interactions are present, they are generally destabilizing or only weakly stabilizing to the closed conformations of the proteins.

On the other hand, although the extent of nonpolar buried surface area between domains in the closed conformations can be extensive (Table 2), it is about as extensive, or even considerably more so, in the open conformations (Table 4) and thereby overcomes the energy penalty incurred by the opening of the domains. Consistently, our calculations indicate that the total nonpolar buried surface area in the open conformation is also roughly as large, or slightly larger, than in the closed conformation (Table 5), although, as expected, the differences are small. Moreover, when the nonpolar surface area buried between the domains in the closed conformation is small, a larger swiveling of the domains is observed, with a consequently lesser extent of buried surface area between the domains in the open conformation. Conversely, when the nonpolar surface area buried between the domains in the closed conformation is large, a smaller opening of the domains is observed, with a consequently larger extent of buried surface area between the domains in the open conformation; this larger buried surface area overcomes the energy penalty involved.

Table 9. Nonpolar Buried Surface Area at the Interface in Mutants (and Additional Conformations[a]) as Compared to Wild Type (Closed Conformation)

		NPBSA[b]				Movement Extents[c]	
Protein	Mutation(s)	Total[d]	Intra[e]	Inter[f]	Bend[g]	Twist[h]	Distance[i]
T-4 Lysozyme Mutants with Increased Stability and Reduced Activity (Hinging Domain: *N–59*)							
1qt6 A	E11h, C54t, C97a	6241	4507	1734	0.166	33.286	−0.322
1qt7 A	E11n, C54t, C97a	6189	4457	1732	6.542	−0.703	1.005
253l	D20a, C54t, C97a	6209	4431	1778	40.552	−22.651	1.104
254l	D20s, C54t, C97a	6155	4401	1754	41.014	−22.474	1.120
255l	D20n, C54t, C97a	6217	4452	1765	41.137	−22.051	1.104
1l36	E128a, V131a, N132a	6210	4465	1745	−1.597	0.309	0.256
1l70	V131a, N132a	6168	4440	1728	−1.653	0.466	0.261
1l73	D127a, E128a, V131a, N132a	6193	4467	1726	8.691	−1.962	1.200
1l74	E128a, V131a, N132a, L133a	6174	4432	1742	−9.976	−15.556	0.238
1l75	D127a, E128a, V131a, N132a, L133a	6187	4452	1732	22.698	−17.485	0.912
1qt5 A	D20e, C54t, C97a	6244	4489	1755	−0.242	34.131	−0.287
1qtz A	D20c, C54t, C97a	6266	4524	1742	40.401	−22.248	1.093
(Total, intra, and inter NPBSA in wild-type are 6162 Å^2, 5353 Å^2 and 16779 Å^2, respectively.)							
HIV Protease (Hinging domain: 33–62)							
Drug-Resistant Mutants							
1gnn A	V82d	2999	1766	1233	−0.614	−8.313	2.535
1gnm A	V82n	3027	1809	1218	53.043	−96.401	4.134
1a30 A	Q7k, L33i, L63i	2997	1757	1240	5.188	2.161	−0.580
1d4s A	V82f, I84v	3077	1790	1287	0.439	−2.647	2.320
1d4y A	Q7k, L33i, L63i	3051	1799	1252	4.141	4.066	−0.473
Additional Structures of Retroviral Proteases[a]							
7hvp A[j]	—	3047	2429	1203	4.227	1.232	3.706
1az5[k]	—	3032	2183	1638	0.922	−17.344	0.100
3hvp[l]	—	3069	2452	1207	−3.219	8.300	−2.871
3phv[m]	—	2920	2313	1146	−0.894	6.735	2.642
1hhp[m]	—	3043	2411	1280	3.172	−17.599	−0.213
(Total, intra, and inter NPBSA in wild-type are 3113 A^2, 2496 Å^2 and 1194 Å^2, respectively.)							

The comparison of nonpolar surface area buried at the hinging-domain interface between wild-type (closed) and mutant structures. The PDB codes of mutant structures are listed. Linear regressions of the change in interdomain nonpolar surface area between the closed and open conformations have also been carried out for the 12 T4 lysozyme mutants. In this case, the change in interdomain nonpolar surface area between the wild-type and the mutant structure ($\Delta ASA^{nonpolar}_{inter} = \Delta ASA^{nonpolar}_{inter\text{-}wild} - \Delta ASA^{nonpolar}_{inter\text{-}mutant}$) shows a weak correlation with distance upon normalization by interdomain nonpolar surface ASA in the mutant structure ($ASA^{nonpolar}_{inter\text{-}mutant}$). The linear correlation coefficient, r, for the T4 lysozyme mutants is 0.6 ($r^2 = 0.36$). Again, the Student's t test shows that this correlation is significant at the 95% level of confidence but not at the 99% level. Combined with the analyses from Table 4, these suggest a possible correlation between the change in interdomain nonpolar surface area and domain movement in proteins. The fact that the Student's t test shows this correlation to be significant indicates that our observations are able to overcome the bias due to the small size of our data.

[a] Other available retroviral protease structures in liganded and unliganded forms were also compared with thereference wild-type structure of HIV protease (4hvp A).

[b] Nonpolar buried surface area.

[c] The movement extents were calculated as described in the legend to Table 2 and in the Experimental Procedures.

[d] Total nonpolar buried surface area of the hinging region.

[e] Nonpolar buried surface area within the hinging region.

[f] Nonpolar buried surface area at the interface of the hinging regions and the rest of the protein.

[g] Bending angle of the hinging domain when wild-type and mutant conformations are compared.

[h] Twisting angle of the hinging domain when wild-type and mutant conformations are compared.

[i] The distance between the centroid of the hinging domain and centroid of the rest of the protein. The distances are wild-type (closed) minus mutant.

[j] Liganded and closed.

[k] SIV protease, open conformation.

[l] Unliganded adn open conformation of HIV protease.

[m] Unliganded HIV protease.

Table 9 further examines available experimental data of mutants, additional conformations, and homologous proteins. Shoichet et al. [45] have analyzed a number of mutants of T4 lysozyme. In all cases that they have probed, although the mutations yielded more-stable structures, the activity of the enzyme was lower, illustrating that too much stability is counter-productive to the enzyme. As the top part of the table shows, in all cases the extent of the nonpolar buried surface area at the interface is increased in the closed conformation. However, the difference (about 50–100 Å^2 more in the mutants as compared to the wild-type) is too small to enable a definitive statement. The bottom part of the table gives cases relating to the HIV protease. The first five cases are drug-resistant mutants [4]. All bury a larger extent of nonpolar surface area in the closed conformations,

although again the differences are not large. Consistently, the structure of SIV, which is in the open conformation [4], buries more nonpolar surface area at the interdomain interface than the corresponding HIV structure. However, the sequences are not identical, so it is difficult to compare directly. The statistical analysis for this table is given in the Table 9 legend.

Biological Implications

Although the trends shown here are qualitative, they nevertheless suggest some general guidelines. Biological function has long been known to relate to hinge-bending motions. Our results indicate that between moving domains there are very few, if any, close-range electrostatic interactions, particularly salt bridges. On the other hand, the nonpolar buried surface area may be extensive. Furthermore, in those cases in which the nonpolar buried surface area between the hinging domains in the closed conformation is large, it is as large or even larger in the open conformation. Interestingly, in such (large nonpolar buried-surface-area) cases, the opening of the domains is not as large as in cases in which the nonpolar buried surface area in the closed conformation is appreciably smaller.

The presence of ligands, like changes in external conditions, leads to a population shift. The protein landscape is dynamic and reflects the redistribution of the conformer population [1, 2, 46]. Hence, conformational transitions are affected by the physiological states. The binding of a ligand/effector stabilizes the bound conformation and leads to conformational transitions in its direction. In this regard, in our limited number of cases, it is of interest to note that enzymes/proteins (e.g., adenylate kinase, calmodulin, DNA polymerase, see Table 4) that are active in multiple paths in the cellular life cycle bury less nonpolar surface area at their interdomain interface and show a larger opening.

These findings may suggest ways to increase/decrease hinge-bending motions by decreasing/increasing the nonpolar buried surface area between the domains or by introducing electrostatic interactions. Moreover, they might possibly suggest a way of predicting the range of likely motions from the closed conformations and hence may be useful in protein design. Furthermore, such predictions may be useful for drug design because larger motions may be indicative of larger pockets and hence may be suggestive of larger, better-fitting drugs. On the other hand, larger interfaces may suggest higher population times for smaller pockets with different shapes and hence may suggest resistance to larger drugs or inhibitors.

Conclusions

Examination of the interactions between two adjoining domains, separated by a hinge, reveals that whereas the nonpolar buried surface areas can be large, the number of salt bridges and hydrogen bonds is quite small. This suggests that in large-scale, slow hinge-bending motions, the rigidifying electrostatic interactions are preferentially selected against, possibly owing to their specificity, reflected in higher barriers. Consistently, a previous large-scale analysis of 222 salt bridges has shown that these tend to occur at close sequence separation and are largely within the building blocks, rather than between them [11]. Calculations of the electrostatic strengths of salt bridges and ion pairs across the moving parts illustrate that their contributions to protein stability are mostly destabilizing or only weakly stabilizing toward the closed conformation of the protein. This observation appears to be reasonable because the presence of strongly stabilizing electrostatic interactions between the moving fragments, domains, or subunits of the protein would tend to constrain protein motion. Such a situation would be counterproductive to protein function.

On the other hand, the hydrophobic energy opposing the opening of the domains can be large. However, it is offset by the favorable, no-less-extensive hydrophobic interactions formed in the open conformations. These are largely the outcome of side-chain rearrangements. Furthermore, the magnitude of the nonpolar surface area between the domains in the closed conformation appears to govern the opening of the domains. If the nonpolar surface area between the domains in the closed conformation is large, then an equally large nonpolar surface area would need to be buried in the open conformation to overcome the energetic cost of opening the domains. This can most straightforwardly be achieved if that movement is not too large. Hence, it appears that the extent of the nonpolar buried surface area between the domains in the closed conformation dictates the extent of opening and, therefore, the distribution of the population of the open conformers around the native state.

Since hinge-bending motions have low barrier heights, the populations of the closed versus the open conformations are a function of their relative stabilities. If the concentration of the ligand in solution is small, the frequently more stable open conformation may prevail. On the other hand, if the concentration of the ligand is high, the energy landscape of the protein will change. Since binding to ligands (or effectors) stabilizes the bound conformation, binding leads to a shift in the equilibrium toward the closed conformation. Similar changes may be observed in response to other external factors, such as pH, temperature, or ionic strength. The population times are the outcome of the physiological conditions that directly affect the conformational transitions.

Experimentally, engineering electrostatic interactions across the interdomain boundary is likely to constrain motion. On the other hand, reduction of nonpolar side-chain interactions (shorter/smaller side chains, smaller interacting fragments) may lead to larger motions.

Experimental Procedures

Assignment of Hinging Parts and Hinges

The moving domains and hinges are as assigned in the database of molecular movements (DMM). The detection of the moving domains and the hinges in DMM is based on first assigning the static core and then estimating the rigid-body rotation of one domain relative to the other by comparing the open and closed conformations of the same protein [3, 47]. For estimating the bending and twisting angles and the differences in the interdomain distances,

the closed and open conformations were superimposed with the program FlexProt (http://bioinfo3d.math.tau.ac.il/FlexProt/). FlexProt is a powerful, automated flexible-structural comparison program. It carries out flexible-structural alignment and detects the potential flexible regions (i.e., locates the hinges) and the rigid domains simultaneously [20]. The distance between the centroid of the hinging domain and the centroid of the rest of the protein in the open conformation is subtracted from such a distance calculated for the closed conformation. This yields an estimate of the changes in interdomain distances accompanying the movements [20].

The Composition of the Databases

We took from the database of molecular motions [3] those cases in which two or more conformations of the same proteins are known and the motion is predominantly of the hinge-bending type. We have further superimposed the protein pairs and visually examined each pair. In June 1999, there were 25 proteins that showed hinge-bending motion and qualified according to our criteria. The atomic coordinates for the proteins were taken from the Protein Data Bank (PDB) [12] files.

Some cases in which hinge-bending motion is detected by comparison of the conformations of homologous proteins (HIV/SIV) or mutant proteins (T4 lysozyme) were also analyzed. Here we picked those cases for which there have been additional experimental studies [4, 45].

To extend and complement the analysis, we have further utilized a database of 36 nonhomologous monomeric proteins to study salt bridges formed within and across hydrophobic folding units (HFUs). The underlying assumption is that contiguous HFUs may swivel with respect to one another. The details of the 36 structure database are given in Kumar and Nussinov [11].

Nonpolar Buried Surface Area

The nonpolar buried surface area was calculated as described by Tsai and Nussinov [37]. Atoms with partial charges less than 0.25 were considered to be nonpolar [37]. The nonpolar buried surface area is the fraction of the total nonpolar area that is buried. To calculate the area buried within the fragment, domain, or subunit or between these and the remainder of the protein, we scrutinized the region for the proportion of its surface area that was buried, both by itself and by the rest of the protein. If a residue in the moving part was buried to the same extent both by a residue within the part and by a residue in the remainder of the protein, the calculated buried surface area for that region was added to both categories. For this reason, in Tables 2 and 4, the total nonpolar buried surface area of the moving part is smaller than the sum of the areas buried by the part and of the area buried by the remainder of the protein.

Hydrophobic Stabilization at the Interface of Hinging Domains

Hydrophobic stabilization at the interface of the hinging domains was estimated via the method suggested by Chothia [48]. This method is based on the observation that the free energy of transferring an amino acid side chain from water to a nonpolar solvent (the hydrophobic effect) is directly proportional to the solvent-accessible surface area of the side chains [49], where 1 $Å^2$ of buried surface corresponds to 25 cal of hydrophobic stabilization. The nonpolar surface area of the hinging domain buried by the rest of the protein is multiplied by 25 and divided by 1000 to estimate the hydrophobic contribution in kcal/mol.

Salt Bridges and Hydrogen Bonds

The definition of a salt bridge was taken from Kumar and Nussinov [11]. According to this definition, two oppositely charged residues are inferred to form a salt bridge if they satisfy the following two criteria: (1) Centroids of side-chain functional groups in oppositely charged residues lie within 4.0 Å of each other [29]; and (2) At least a pair of Asp or Glu side-chain carboxyl oxygen and Arg, Lys, and His side-chain nitrogen atoms are within a 4.0 Å distance. The presence of a hydrogen bond is inferred when two non-hydrogen atoms with opposite partial charges are within a distance of 3.5 Å.

Electrostatic Strength Calculations for Salt Bridges and Ion Pairs

Electrostatic strengths of salt bridges in protein crystal structures are calculated with the continuum electrostatic methodology [11, 30, 39]. The electrostatic contribution to the free energy change upon salt bridge formation is calculated relative to computer mutations of the salt-bridging residue's side chains to their hydrophobic isosteres. The hydrophobic isosteres are the salt-bridging residue's side chains with their partial atomic charges set to zero.

$\Delta\Delta G_{tot}$, the total electrostatic contribution to the free-energy change upon formation of a salt bridge, is the sum of three components: $\Delta\Delta G_{tot} = \Delta\Delta G_{dslv} + \Delta\Delta G_{brd} + \Delta\Delta G_{prt}$. $\Delta\Delta G_{dslv}$ is the sum of the unfavorable desolvation penalties incurred by the individual salt-bridging residues due to the change in their environment from a high dielectric solvent (water) in the unfolded state to the low dielectric protein interior in the folded state of the protein. $\Delta\Delta G_{brd}$ is the favorable bridge energy due to the electrostatic interaction of the side chain charged groups with each other in the folded state of the protein. $\Delta\Delta G_{prt}$ is the electrostatic interaction of the salt-bridging side chains with the charges in the rest of the protein in the folded state.

An additional free-energy term called association energy, $\Delta\Delta G_{assoc}$, represents the desolvation of the salt bridge and the electrostatic interaction between the salt-bridging side chains but does not consider the electrostatic interaction of the salt bridge with the rest of the protein. Hence, it represents the electrostatic contribution to the free-energy change upon salt bridge formation in the absence of charges in the rest of the protein [39]. All of the energy values are presented in kcal/mol. All of the calculations were performed with the DELPHI package [50–54]. This method has been used extensively earlier [11, 30, 31, 39, 55], and experimental support for this method has been reported [56, 57]. The details of the method used here are given in Kumar and Nussinov [11] and Kumar et al. [30]. In all calculations, the solute (protein) dielectric is 4.0, and the solvent (water) dielectric is 80.0. The electrostatic strength calculations for ion pair networks were performed in a similar manner. All hydrogen atoms were added to the structures, and the protonation states of the charged residues were defined at pH 7.0 with the BIOPOLYMER module of INSIGHT II. The PARSE3 set of atomic charges and radii [58] and a solvent probe radius of 1.4 Å were used. The output energy value in units kT, where k is the Boltzman constant and T is the absolute temperature, were multiplied with the conversion factor 0.592 to obtain the results in kilocalories per mole at room temperature (25°C). For each calculation, the structures were first mapped onto the grid, where the molecules occupied 25%–50% of the grid and Debye-Huckel boundary conditions were applied [59]. The resulting rough calculations were used as a boundary condition for the focused calculation, where 95% of the grid is occupied by the protein molecule and the remaining 5% is water. The results of focused calculations are shown here.

Acknowledgments

We thank Drs. Buyong Ma, Jacob V. Maizel, and in particular, Chung-Jung Tsai for numerous helpful and insightful discussions. Advanced Biomedical Computing Center personnel are thanked for computational resources and related assistance. The personnel at NCI-Frederick are thanked for their assistance. The research of R.N. in Israel has been supported in part by grant number 95-00208 from BSF, Israel; by a grant from the Ministry of Science; by the Center of Excellence, administered by the Israel Academy of Sciences; by the Magnet grant; and by the Tel Aviv University Basic Research and Adams Brain Center grants. This project has been funded in whole or in part with federal funds from the National Cancer Institute, National Institutes of Health, under contract number NO1-CO-56000. The content of this publication does not necessarily reflect the view or policies of the Department of Health and Human Services, nor does mention of trade names, commercial products, or organization imply endorsement by the U.S. Government.

Received: May 22, 2001
Revised: September 6, 2001
Accepted: October 23, 2001

References

1. Ma, B., Kumar, S., Tsai, C.J., and Nussinov, R. (1999). Folding funnels and binding mechanisms. Protein Eng. *12*, 713–720.
2. Kumar, S., Ma, B., Tsai, C.J., Sinha, N., and Nussinov, R. (2000). Folding and binding cascades: dynamic landscapes and population shifts. Protein Sci. *9*, 10–19.
3. Gerstein, M., and Krebs, W. (1998). A database of macromolecular motions. Nucleic Acids Res. *26*, 4280–4290.
4. Rose, R.B., Craik, C.S., and Stroud, R.M. (1998). Domain flexibility in retroviral proteases: structural implications for drug resistant mutations. Biochemistry *37*, 2607–2621.
5. Collins, J.R., Burt, S.K., and Erickson, J.W. (1995). Flap opening in HIV-1 protease simulated by 'activated' molecular dynamics. Nat. Struct. Biol. *2*, 334–338.
6. Erickson, J.W., Baldwin, E.T., Bhat, T.N., and Gulik, S. (1995). Structure of human cathepsin D: comparison of inhibitor binding and subdomain displacement with other aspartic proteases. In Aspartic Proteinases: Structure, Function, Biology and Biomedical Implications, K. Takahashi, ed. (New York: Plenum Press).
7. Sali, A., Cooper, J.B., Foundling, S.I., Hoover, D.J., and Blundell, T.L. (1989). High-resolution X-ray diffraction study of the complex between endothiapepsin and an oligomer inhibitor: the analysis of the inhibitor binding and description of the rigid body shift in the enzyme. EMBO J. *8*, 2179–2188.
8. Lee, A.Y., Gulnik, S.V., and Erickson, J.W. (1998). Conformational switching in an aspartic proteinase. Nat. Struct. Biol. *5*, 866–871.
9. Muller, Y., Kelley, R.F., and De Vos, A.M. (1998). Hinge bending within the cytokine receptor superfamily revealed by the 2.4 Å crystal structure of the extracellular domain of the rabbit tissue factor. Protein Sci. *7*, 1106–1115.
10. Keskin, O., Jernigan, R.L., and Bahar, I. (2000). Proteins with similar architecture exhibit similar large-scale dynamic behavior. Biophys. J. *78*, 2093–2106.
11. Kumar, S., and Nussinov, R. (1999). Salt bridge stability in monomeric proteins. J. Mol. Biol. *293*, 1241–1255.
12. Bernstein, F.C., et al., and Tasumi, M. (1977). The protein databank: a computer-based archival file for macromolecular structures. J. Mol. Biol. *112*, 535–542.
13. Sandak, B., Nussinov, R., and Wolfson, H. (1995). An automated computer-vision & robotics based technique for 3-D flexible biomolecular docking and matching. Comput. Appl. BioSci. *11*, 87–99.
14. Sandak, B., Wolfson, H., and Nussinov, R. (1998). Flexible docking allowing induced fit in proteins: insights from open to closed conformational isomers. Proteins Struct. Funct. Genet. *32*, 159–174.
15. Wriggers, W., and Schulten, K. (1997). Protein domain movements: Detection of rigid domains and visualization of hinges in comparisons of atomic coordinates. Proteins Struct. Funct. Genet. *29*, 1–14.
16. Verbitsky, G., Nussinov, R., and Wolfson, H. (1999). Flexible structural comparison allowing hinge-bending, swiveling motions. Proteins Struct. Funct. Genet. *34*, 232–254.
17. de Groot, B.L., Hayward, S., van Aalten, D.M.F., Amadi, A., and Berendsen, H.J.C. (1998). Domain motions in bacteriophage T4 lysozyme: a comparison between molecular dynamics and crystallographic data. Proteins Struct Funct. Genet *31*, 116–127.
18. Wernisch, L., Hunting, M., and Wodak, S.J. (1999). Identification of structural domains in proteins by graph heuristic. Proteins Struct. Funct. Genet. *35*, 338–352.
19. Hayward, S. (1999). Structural principles governing domain motions in proteins. Proteins Struct. Funct. Genet. *36*, 425–435.
20. Shatsky, M., Fligelman, Z., Nussinov, R., and Wolfson, H. (2000). Alignment of flexible protein structures. In Proceedings of the 8th Conference on Intelligent Systems in Molecular Biology (ISMB), Altman et al., eds. (Menlo Park, CA: AAAI Press), pp. 329–343.
21. Hayward, S., Kitao, A., and Berendsen, H.J. (1997). Model free methods to analyze domain motions in proteins from simulation. A comparison of a normal mode analysis and a molecular dynamics simulation of lysozyme. Proteins Struct. Funct. Genet. *27*, 425–437.
22. Hayward, S., and Berendsen, H.J. (1998). Systematic analysis of domain motions in proteins from conformational change: new results on citrate synthase and T4 lysozyme. Proteins Struct. Funct. Genet. *30*, 144–154.
23. Bahar, I., Erman, B., Haliloglu, T., and Jernigan, R.L. (1997). Identification of cooperative motions and correlated structural elements in coarse-grained proteins. Application to T4 lysozyme. Biochemistry *36*, 13512–13523.
24. Sun, J., and Sampson, N.S. (1998). Determination of the amino acid requirements for a protein hinge in triosephosphate isomerase. Protein Sci. *7*, 1495–1505.
25. Gerstein, M., Lesk, A., and Chothia, C. (1994). Structural mechanism for domain movements in proteins. Biochemistry *33*, 6739–6749.
26. Tsai, C.J., Kumar, S., Ma, B., and Nussinov, R. (1999). Folding funnels, binding funnels and protein function. Protein Sci. *8*, 1181–1190.
27. Creighton, T.E. (1993). Proteins: Structures and Molecular Properties, Second Edition (New York: W.H. Freeman and Company), p. 142.
28. Tsai, C.J., Lin, S.L., Wolfson, H.J., and Nussinov, R. (1997). Studies of protein-protein interfaces: a statistical analysis of the hydrophobic effect. Protein Sci. *6*, 53–64.
29. Barlow, B.J., and Thornton, J.M. (1983). Ion-pairs in proteins. J. Mol. Biol. *168*, 867–885.
30. Kumar, S., Ma, B., Tsai, C.J., and Nussinov, R. (2000). Electrostatic strengths of salt bridges in thermophilic and mesophilic glutamate dehydrogenase monomers. Proteins Struct. Funct. Genet. *38*, 368–383.
31. Xu, D., Tsai, C.J., and Nussinov, R. (1997). Hydrogen bonds and salt bridges across protein-protein interfaces. Protein Eng. *10*, 999–1012.
32. Perutz, M.F. (1970). Stereochemistry of cooperative effects in haemoglobin. Nature *228*, 726–739.
33. Fersht, A.R. (1972). Conformational equilibria in α- and δ-chymotrypsin. The energetics and importance of the salt bridge. J. Mol. Biol. *64*, 497–509.
34. Warshel, A., Naray-Szabo, G., Sussman, F., and Hwang, J.K. (1989). How do serine proteases really work? Biochemistry *28*, 3629–3637.
35. Musafia, B., Buchner, V., and Arad, D. (1995). Complex salt bridges in proteins: statistical analysis of structure and function. J. Mol. Biol. *254*, 761–770.
36. Kumar, S., Tsai, C.J., and Nussinov, R. (2000). Factors enhancing protein thermostability. Protein Eng. *13*, 179–191.
37. Tsai, C.J., and Nussinov, R. (1997). Hydrophobic folding units derived from dissimilar monomer structures and their interactions. Protein Sci. *6*, 24–42.
38. Kumar, S., and Bansal, M. (1998). Dissecting α-helices: position specific analysis of α-helices in globular proteins. Proteins Struct. Funct. Genet. *31*, 460–476.
39. Hendsch, Z.S., and Tidor, B. (1994). Do salt bridges stabilize proteins? A continuum electrostatic analysis. Protein Sci. *3*, 211–226.
40. Koshland, D.E., Jr. (1958). Application of a theory of enzyme specificity to protein synthesis. Proc. Natl. Acad. Sci. USA *44*, 98–123.
41. Dill, K.A. (1990). Dominant forces in protein folding. Biochemistry *31*, 7134–7155.
42. Xu, D., Lin, S.L., and Nussinov, R. (1997). Protein binding versus protein folding: the role of hydrophilic bridges in protein associations. J. Mol. Biol. *265*, 68–84.
43. Sinha, N., Tsai, C.J., and Nussinov, R. (2001). A proposed structural model for amyloid fibril elongation: domain swapping forms an interdigitating β-structure polymer. Protein Eng. *14*, 93–103.
44. Kumar, S., and Nussinov, R. (2001). Fluctuations between stabilizing and destabilizing electrostatic contributions of ion pairs in conformers of the c-Myc-Max leucine zipper. Proteins Struct. Funct. Genet. *41*, 485–497.
45. Shoichet, B.K., Baase, W.A., Kuroki, R., and Matthews, B.W. (1995). A relationship between protein stability and protein function. Proc. Natl. Acad. Sci. USA *92*, 452–456.
46. Tsai, C.J., Ma, B., and Nussinov, R. (1999). Folding and binding

cascades: shifts in energy landscapes. Proc. Natl. Acad. Sci. USA *96*, 9970–9972.
47. Gerstein, M., Anderson, B.F., Norris, G.E., Baker, E.N., Lesk, A.M., and Chothia, C. (1993). Domain closure in lactoferrin. Two hinges produce a see-saw motion between alternative close-packed interfaces. J. Mol. Biol. *234*, 357–372.
48. Chothia, C. (1974). Hydrophobic bonding and accessible surface area in proteins. Nature *248*, 338–339.
49. Rose, G.D., Geselowitz, A.R., Lesser, G.J., Lee, R.H., and Zehfus, M.H. (1985). Hydrophobicity of amino acid residues in globular proteins. Science *229*, 834–838.
50. Gilson, M.K., Rashin, A., Fine, R., and Honig, B. (1985). On the calculation of electrostatic interactions in proteins. J. Mol. Biol. *183*, 503–516.
51. Gilson, M.K., Sharp, K.A., and Honig, B.H. (1988). Calculating the electrostatic potential of molecules in solution: method and error assessment. J. Comp. Chem. *9*, 327–335.
52. Gilson, M.K., and Honig, B.H. (1987). Calculation of electrostatic potential in an enzyme active site. Nature *330*, 84–86.
53. Gilson, M.K., and Honig, B.H. (1988). Calculation of the total electrostatic energy of a macromolecular system: solvation energies, binding energies, and conformational analysis. Proteins Struct. Funct. Genet. *4*, 7–18.
54. Honig, B., Sharp, K., and Yang, A. (1993). Macroscopic models of aqueous solutions: biological and chemical applications. J. Phys. Chem. *97*, 1101–1109.
55. Lounnas, V., and Wade, R.C. (1997). Exceptionally stable salt bridges in cytochrome P450cam have functional roles. Biochemistry *36*, 5402–5417.
56. Waldburger, C.D., Schildbach, J.F., and Sauer, R.T. (1995). Are buried salt bridges important for protein stability and conformational specificity? Nat. Struct. Biol. *2*, 122–128.
57. Waldburger, C.D., Jonsson, T., and Sauer, R.T. (1996). Barriers to protein folding: formation of buried polar interactions is a slow step in acquisition of structure. Biochemistry *93*, 2629–2634.
58. Sitkoff, D., Sharp, K.A., and Honig, B. (1994). Accurate calculation of hydration free energies using macroscopic solvent models. J. Phys. Chem. *98*, 1978–1988.
59. Klapper, I., Hagstrom, R., Fine, R., Sharp, K., and Honig, B. (1986). Focusing of electric fields in the active site of Cu-Zn superoxide dismutase: effects ionic strength and amino acid modification. Proteins Struct. Funct. Genet. *1*, 47–59.
60. Nicholls, A., Sharp, K.A., and Honig, B. (1991). Protein folding and association: insights from the interfacial and thermodynamic properties of hydrocarbons. Proteins Struct. Funct. Genet. *11*, 281–296.

Note Added in Proof

After submission of our paper, further experimental evidence supporting our conclusions has appeared [Wooll et al. (2001). J. Mol. Biol. *312*, 525-540]. The authors have observed that upon the loss of an intersubunit salt bridge between Asp177 of domain B and Arg341 of domain A of the second subunit, there is an increased rotational flexibility of domain B, which contains the binding site. The functional role of this intersubunit salt bridge is proposed to determine the conformational distribution between R and T states of pyruvate kinase. Whereas here the authors have observed the effect on the subunit motions and we focus on domain motion, the same principles nevertheless apply.